Supplementary Material

Diagnosing the Controls of the 2025 Talidas GLOF Using Multi-Source Satellite Observations

Imran Khan[1,2], Jeremy M. Johnston[1,2], and Jennifer M. Jacobs[1,2]

[1]Department of Civil and Environmental Engineering, University of New Hampshire, Durham, NH 03824, United States

[2]Earth Systems Research Center, Institute for the Study of Earth, Oceans, and Space, University of New Hampshire, Durham, NH 03824, United States

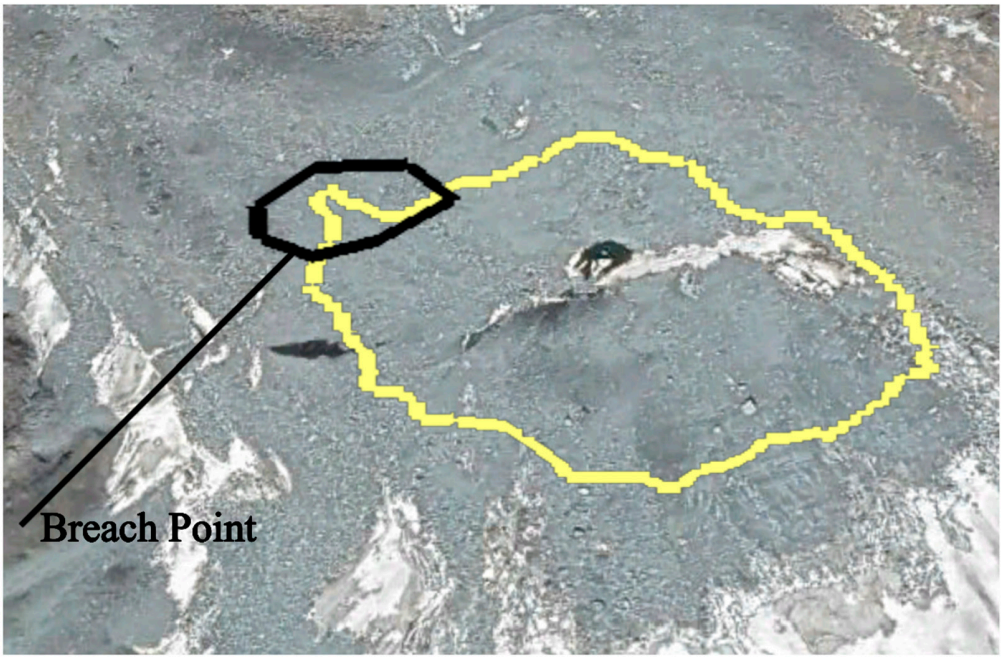


Figure S1. Google Earth image showing the lake basin, composed of morphologically heterogeneous and rough surface material, predominantly coarse and poorly sorted sediment composition, likely consisting of a mixture of boulders, cobbles, and finer material.

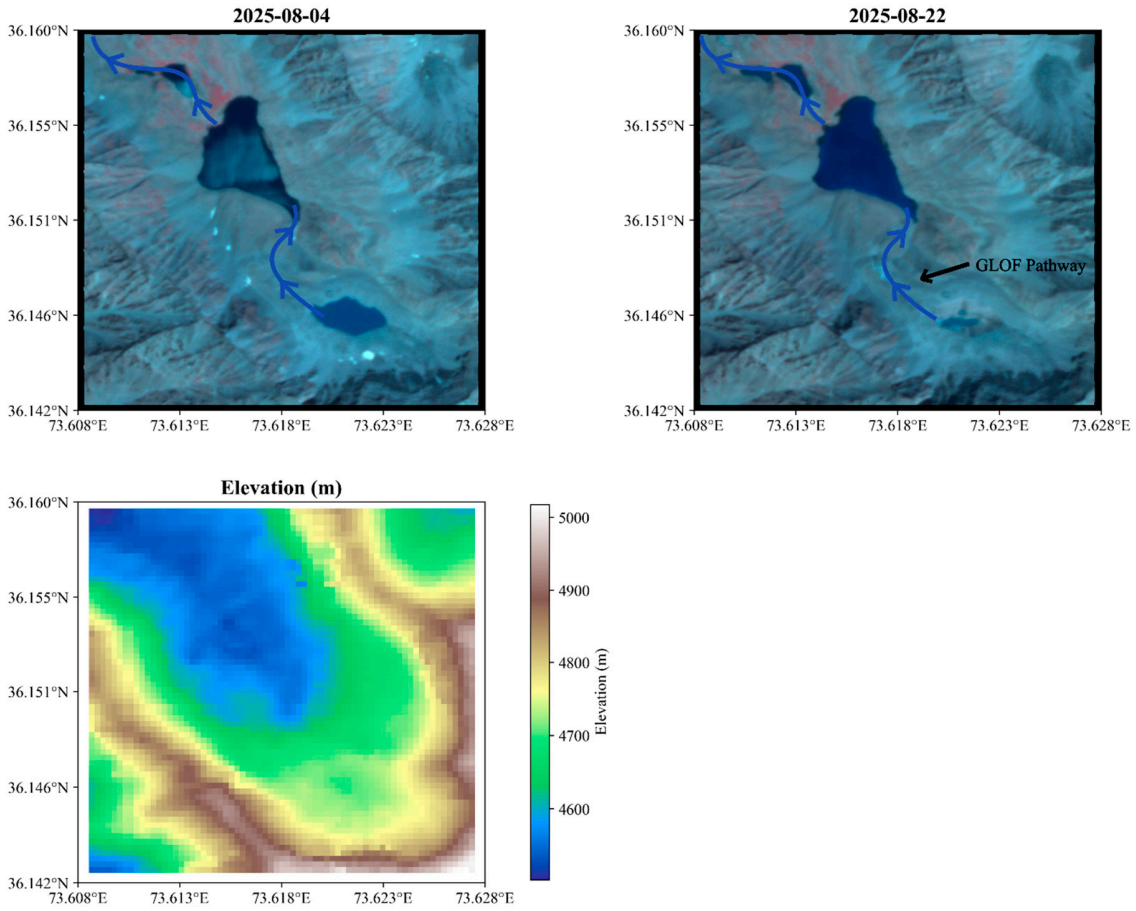


Figure S2. False color composite of PlanetScope image from August 04, 2025, showing multiple lakes upstream of the Talidas settlement. The lake at the highest elevation drained out on August 22, 2025, while the lakes below overflowed due to the flood wave but remained structurally intact and did not undergo catastrophic drainage.

Table S1. Summary of remote sensing and reanalysis datasets used in this study, including sensor/source, temporal coverage, spatial resolution, and specific applications in the study.

Dataset	Sensor/Source	Time Period	Spatial Scale	Usage
PlanetScope Multispectral Imagery (Level 3B Ortho Scene Analytic)	Planet Labs (Planet Explorer, E&R License)	Lake and SCA mapping: 2022-2025, and visual observation: 2016-2021	3 m	Mapping seasonal glacial lake extent and SCA within the lake catchment.
Landsat 5 TM, Landsat 7 ETM+, Landsat 8-9 OLI	United States Geological Survey (via Google Earth Engine)	1992-2018	30 m	Reconstruction of historical lake presence, extent, and long-term lake dynamics.

MODIS Terra Global Snow Cover Product	MODIS Terra / National Snow and Ice Data Center	2000-2025 (June to September)	0.01 Degrees (1.1 km)	Deriving snow presence/absence and snow persistence dynamics within the lake catchment.
SRTM Digital Elevation Model	NASA SRTM via Google Earth Engine	2000	30 m	Derivation of elevation, slope, and topographic characteristics of the lake catchment.
ERA5-Land Reanalysis Daily Average Temperature and Total Precipitation	ECMWF (via Google Earth Engine)	2000-2025 (daily average temperature) and August 2025 (daily total precipitation)	0.1 Degrees (~9 km)	Analysis of melt-season temperature variability, and precipitation conditions preceding the GLOF.
GPM IMERG (Version 7) Daily Total Precipitation	NASA Global Precipitation Measurement via Google Earth Engine	August 2025	0.1 Degrees (~10 km)	Assessment of precipitation during the pre-event period.
HMA Permafrost Dataset	MODIS-AIRS / National Snow and Ice Data Center	2003-2016	1 km	Assessment of permafrost probability

Table S2. Performance metrics for independent temporal validation of the Random Forest snow classification using manually digitized validation polygons from June 20, July 2, and July 21, 2025.

Class	**Precision**	**Recall**	**F-1 Score**
1 (Snow)	0.93	1.00	0.96
2 (Debris and Rock)	1.00	0.94	0.97
3 (Water)	1.00	1.00	1.00

Independent temporal validation of the Random Forest classifier using manually digitized polygons from June 20, July 2, and July 21, 2025, indicates strong classification performance across all land-cover classes. The model achieved an overall accuracy of approximately 99%, demonstrating robust transferability to imagery not used during training. The results demonstrate

that the RF-based approach provides accurate and consistent discrimination between snow and non-snow surfaces in high-resolution PlanetScope imagery.

Table S3. Lake area and volume change during summer 2025. Lake volume is estimated using the empirical equation suggested by Cook and Quincey 2015.

Date	**Area (m^2)**	**Area (km^2)**	**Area Uncertainty**	**Volume (m^3)**
19-Jun-25	11815.29	0.0118	0.0006	69063.26
20-Jun-25	14076.87	0.0141	0.0006	88453.43
23-Jun-25	18580.08	0.0186	0.0008	130926.60
24-Jun-25	20449.80	0.0205	0.0008	149921.25
3-Jul-25	31257.95	0.0313	0.0010	273036.19
9-Jul-25	34913.21	0.0349	0.0010	319213.20
21-Jul-25	39758.74	0.0398	0.0011	383556.13
29-Jul-25	42947.52	0.0429	0.0010	427729.14
3-Aug-25	45122.51	0.0451	0.0011	458651.41
16-Aug-25	49120.56	0.0491	0.0011	517102.30
20-Aug-25	51997.24	0.0520	0.0011	560401.30
22-Aug-25	7679.18	0.0077	0.0004	37570.93

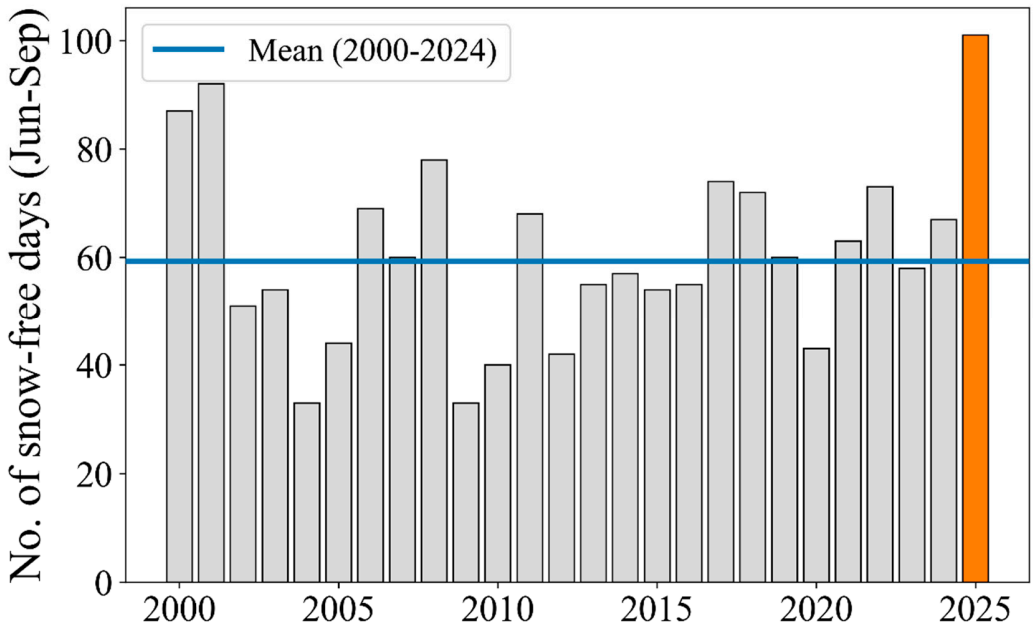


Figure S3. Number of snow-free days in the lake catchment during the June-September period for 2000-2025 derived from MODIS observations. The horizontal blue line indicates the mean number of snow-free days for the 2000-2024 baseline. The chart shows that 2025 experienced the highest number of snow-free days in the 26-year record, reflecting exceptionally early and sustained seasonal snow depletion.

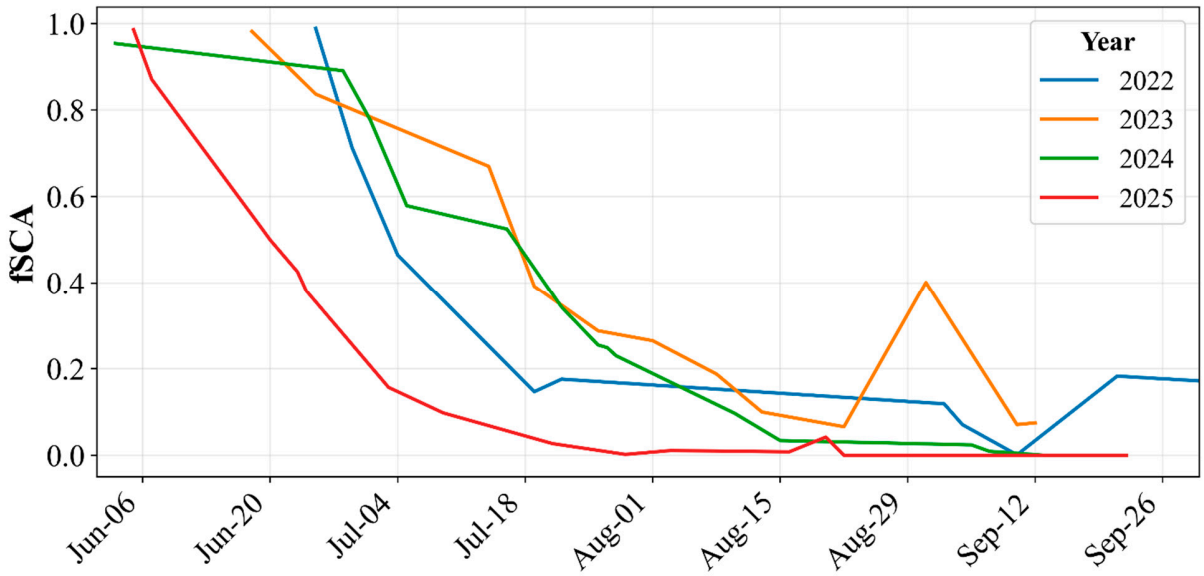


Figure S4. Seasonal evolution of fSCA within the lake catchment for the 2022-2025 melt seasons. All years show rapid snow depletion during early summer followed by low and stable values in July-August. The 2025 season exhibits consistently lower fSCA and earlier transition to near-snow-free conditions compared to the preceding years.

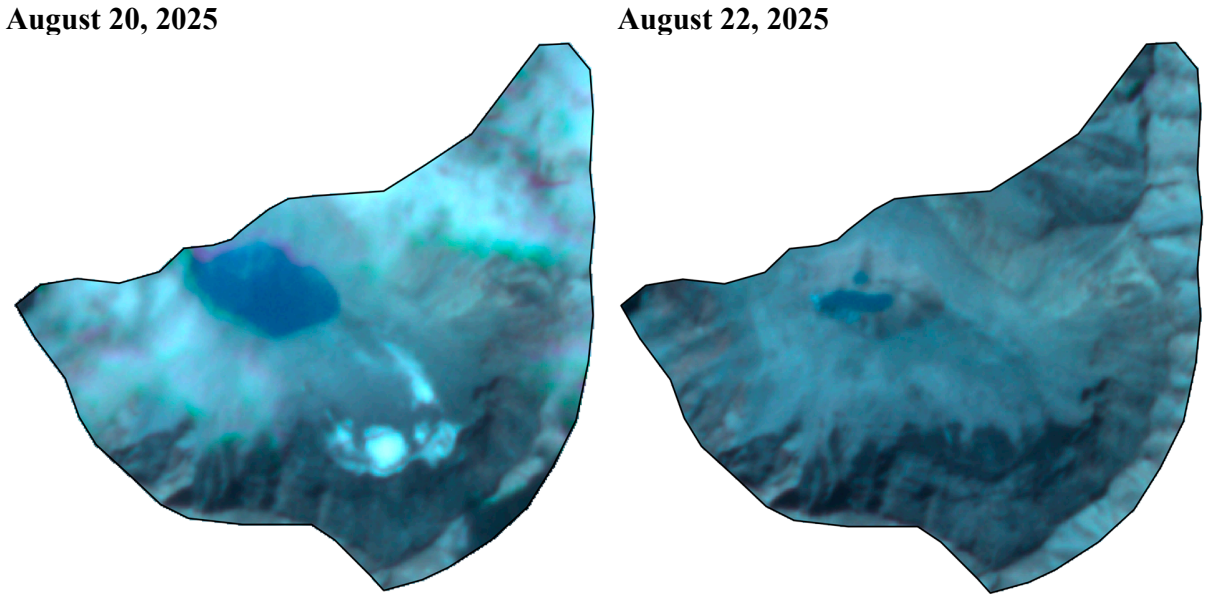


Figure S5. False color composite of PlanetScope image from August 20, 2025, showing fresh snow on the higher elevation slope upstream of the lake, which disappeared in addition to the drainage of the lake by the August 22, 2025, image.

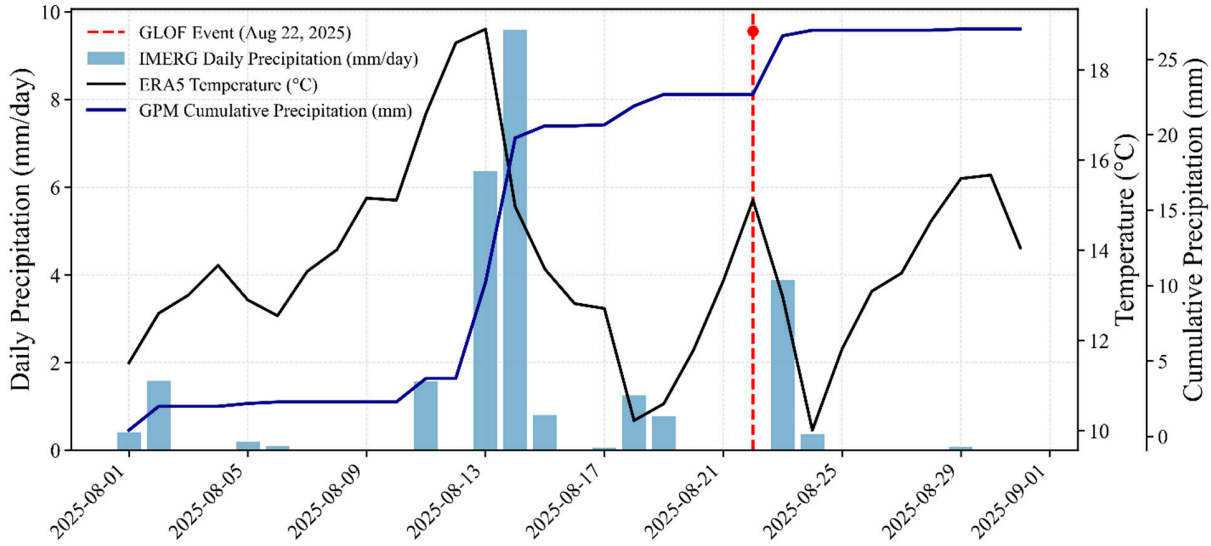


Figure S6. Daily areal-mean precipitation over the lake catchment during August 2025 derived from GPM IMERG V07 dataset and daily temperature derived from ERA5-Land dataset. The precipitation pulses preceding the outburst suggest additional short-term hydrometeorological inflow and moist soil.